Ala^{657} and Conserved Active Site Residues Promote Fibroblast Activation Protein Endopeptidase Activity via Distinct Mechanisms of Transition State Stabilization

Sarah A. Meadows,[‡] Conrad Yap Edosada,[‡] Mark Mayeda,[‡] Thuy Tran,[§] Clifford Quan,[§] Helga Raab,[||] Christian Wiesmann,[⊥] and Beni B. Wolf*[,‡]

Departments of Molecular Oncology, Medicinal Chemistry, Protein Chemistry, and Protein Engineering, Genentech, Inc., South San Francisco, California 94080

Received October 26, 2006; Revised Manuscript Received February 20, 2007

ABSTRACT: Fibroblast activation protein (FAP) and dipeptidyl peptidase-4 (DPP-4) are highly homologous serine proteases of the prolyl peptidase family and therapeutic targets for cancer and diabetes, respectively. Both proteases display dipeptidyl peptidase activity, but FAP alone has endopeptidase activity. FAP Ala^{657}, which corresponds to DPP-4 Asp^{663}, is important for endopeptidase activity; however, its specific role remains unclear, and it is unknown whether conserved DPP-4 substrate binding residues support FAP endopeptidase activity. Using site-directed mutagenesis and kinetic analyses, we show here that Ala^{657} and five conserved active site residues (Arg^{123}, Glu^{203}, Glu^{204}, Tyr^{656}, and Asn^{704}) promote FAP endopeptidase activity via distinct mechanisms of transition state stabilization (TSS). The conserved residues provide marked TSS energy for both endopeptidase and dipeptidyl peptidase substrates, and structural modeling supports their function in binding both substrates. Ala^{657} also stabilizes endopeptidase substrate binding and additionally dictates FAP reactivity with transition state inhibitors, allowing tight interaction with tetrahedral intermediate analogues but not acyl−enzyme analogues. Conversely, DPP-4 Asp^{663} stabilizes dipeptidyl peptidase substrate binding and permits tight interaction with both transition state analogues. Structural modeling suggests that FAP Ala^{657} and DPP-4 Asp^{663} confer their contrasting effects on TSS by modulating the conformation of conserved residues FAP Glu^{204} and DPP-4 Glu^{206}. FAP therefore requires the combined function of Ala^{657} and the conserved residues for endopeptidase activity.

Dipeptidyl peptidase-4 (DPP-4) and fibroblast activation protein (FAP)[1] are highly related serine proteases belonging to the prolyl peptidase family, which typically cleaves peptide substrates following proline residues (reviewed in ref *1*). DPP-4 is ubiquitously expressed in normal tissues and is an important therapeutic target for diabetes because it cleaves and inactivates insulinotropic peptides (reviewed in ref *2*). In contrast, FAP shows little normal tissue expression, and endogenous FAP substrates remain largely unknown (*1*). However, FAP is a promising therapeutic target for cancer because stromal fibroblasts in most malignancies express FAP strongly (*3*−*5*), and FAP activity promotes tumorigenesis in preclinical models (*6*, *7*).

The sequences of FAP and DPP-4 are highly identical, and both are type II transmembrane proteins that contain a short cytoplasmic tail, a 20-amino acid transmembrane domain and an ∼740-amino acid extracellular region, which contains an N-terminal β-propeller domain and a C-terminal $\alpha\beta$-hydrolase domain (*8*−*14*). The β-propeller likely regulates access of the substrate to the $\alpha\beta$-hydrolase domain, which contains the catalytic Ser, Asp, and His residues. The proteases require dimerization for activity (*4*, *8*−*17*), and each cleaves peptide substrates via dipeptidyl peptidase activity that removes P_2-Pro$_1$ dipeptides (P_2 represents any amino acid) from the N-terminus of the substrate. FAP additionally has endopeptidase activity against substrates containing a Gly$_2$-Pro$_1$ motif (*18*), which differentiates it from DPP-4.

Crystallographic data with substrates and/or inhibitors bound to DPP-4 (*9*−*14*) have defined key interactions for dipeptidyl peptidase substrate binding. The inhibitor's positively charged N-terminus binds the negatively charged carboxylate side chains of Glu^{205} and Glu^{206} and the hydroxyl group of Tyr^{662} (Figure 1A,B). Neutralization of the substrate's positively charged N-terminus (*19*, *20*) or mutation of Glu^{205} or Glu^{206} (*21*) markedly decreases dipeptidyl peptidase activity, highlighting the importance of these charge−charge interactions. Arg^{125} and Asn^{710} are also important for dipeptidyl peptidase activity, with Asn^{710} directly binding the inhibitor's P_2 carbonyl oxygen and Arg^{125} positioning Glu^{205} for inhibitor binding. Arg^{125} may also directly bind the inhibitor's P_2 carbonyl oxygen after slight rotation. The protease does not bind the side chain of the inhibitor's P_2 residue because it points away from the active site.

Although the FAP crystal structure was determined without a bound substrate (*8*), it shows that the DPP-4 substrate-binding residues are conserved and similarly positioned at

* To whom correspondence should be addressed: Genentech, Inc., 1 DNA Way-MS42, South San Francisco, CA 94080. Telephone: (650) 467-1954. Fax: (650) 467-8195. E-mail: bbwolf@gene.com.

[‡] Department of Molecular Oncology.

[§] Department of Medicinal Chemistry.

[||] Department of Protein Chemistry.

[⊥] Department of Protein Engineering.

[1] Abbreviations: FAP, fibroblast activation protein; DPP, dipeptidyl peptidase; Ac, acetyl; AFC, 7-amino-4-trifluoromethylcoumarin; boro-Pro, proline-boronic acid; TSS, transition state stabilization; WT, wild type.

10.1021/bi062227y CCC: $37.00
Published on Web 03/24/2007

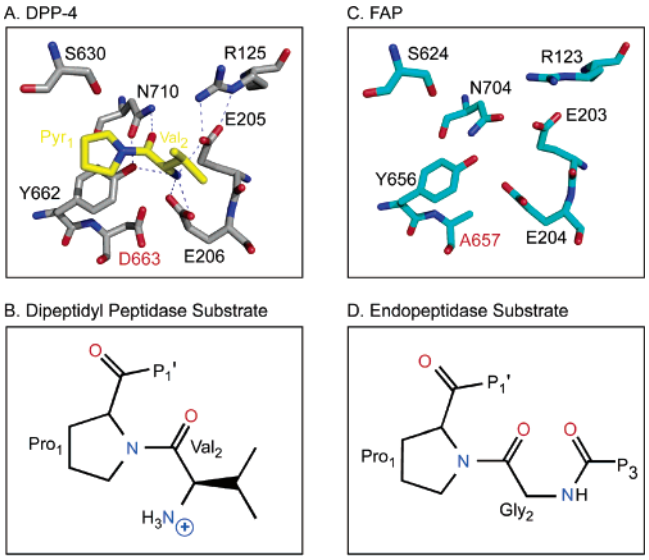

FIGURE 1: Substrate and protease structural models. (A) Structure of DPP-4 bound to the dipeptide inhibitor, Val-pyrrolidide [PDB entry 1n1m (*9*)]. DPP-4 carbon atoms are colored gray, inhibitor carbon atoms yellow, oxygen atoms red, and nitrogen atoms blue. The catalytic serine (Ser^{630}) and substrate binding residues are labeled in black, and the nonconserved residue, Asp^{663}, is labeled in red. (B) Val_2-Pro_1-P_1' as a representative dipeptidyl peptidase substrate. Substrate cleavage occurs between the Pro_1-P_1' bond, where P_1' represents any amino acid. (C) A model of the FAP active site based on the FAP crystal structure [PDB entry 1z68 (*8*)], which was determined without a bound inhibitor. The color scheme is the same as in panel A, except that carbon atoms are colored cyan. (D) P_3-Gly_2-Pro_1-P_1' as a representative endopeptidase substrate. Note that the P_3 residue (P_3 represents any amino acid) replaces the positively charged N-terminus of the dipeptidyl peptidase substrate.

the FAP active site (Figure 1C). These structural similarities and mutagenesis studies with Glu^{203} and Glu^{204} (*22*) suggest that FAP binds dipeptidyl peptidase substrates in a manner similar to that of DPP-4. However, kinetic data are not available for the Glu^{203} and Glu^{204} mutants, and it is unknown whether the glutamates and other conserved residues bind endopeptidase substrates, which lack a charged N-terminus (Figure 1D). The function of Ala^{657} (DPP-4 Asp^{663}), a nonconserved residue near the active site, also remains unclear (Figure 1). Aertgeerts et al. interchanged the Ala and Asp residues and found that Asp at position 657 or 663 potentiates dipeptidyl peptidase activity, whereas Ala at this position allows endopeptidase activity (*8*). These authors suggest that the Asp residue potentiates dipeptidyl peptidase activity by increasing the affinity of protease for the positively charged N-terminus of dipeptidyl peptidase substrates; however, it is unclear how Ala^{657} permits FAP endopeptidase activity.

Using site-directed mutagenesis, kinetic analyses, and structural modeling, we show here that Ala^{657} and five conserved active site residues (Arg^{123}, Glu^{203}, Glu^{204}, Tyr^{656}, and Asn^{704}) promote FAP endopeptidase activity via distinct mechanisms of transition state stabilization (TSS). The conserved residues bind substrate, whereas Ala^{657} allows Glu^{204} to assume a conformation that stabilizes transition state binding of endopeptidase substrates. This conformational effect additionally dictates FAP reactivity with transition state inhibitors, allowing tight interaction with tetrahedral intermediate analogues but not acyl−enzyme analogues. These results provide insight into how Ala^{657} regulates FAP specificity and have implications for rational design of FAP inhibitors.

EXPERIMENTAL PROCEDURES

Materials. Gly-Pro-7-amino-4-trifluoromethylcoumarin (AFC) and acetyl (Ac)-Gly-Pro-AFC were from MP Biomedicals. Proline-boronic acid (boroPro) and proline-nitrile inhibitors were synthesized as described previously (*23*, *24*), purified by reverse phase chromatography, and verified by matrix-assisted laser desorption ionization mass spectrometry.

Site-Directed Mutagenesis. Point mutations were created using the Stratagene Quick Change II XL site-directed mutagenesis kit and verified by DNA sequencing. Primer sequences are listed in Table 1 of the Supporting Information. The final constructs encoded soluble, N-terminally FLAG-tagged versions of FAP (amino acids 38−760) and DPP-4 (amino acids 39−766).

Protease Expression and Characterization. Proteases were expressed in 293 HEK cells, purified from serum-free conditioned medium by anti-FLAG affinity chromatography, and analyzed by SDS−PAGE and gel filtration chromatography coupled with multiangle light scattering for assessing purity and dimer content (*20*). The dimeric fraction was considered the proportion of active protease in each preparation (*15*, *17*).

Protease Kinetics. Protease assays were conducted as described previously (*20*), and kinetic parameters (k_{cat} and K_m) were calculated from Michaelis−Menten plots with nonlinear regression analysis using GraphPad Prism 4. When saturating amounts of substrate could not be achieved, K_m values were estimated from curvilinear substrate−velocity curves and catalytic efficiencies (k_{cat}/K_m) were determined under pseudo-first-order conditions (*20*). Changes in transition state stabilization energy ($\Delta\Delta G_T^{\ddagger}$) for mutant proteases were calculated according to the following equation:

$$\Delta\Delta G_T^{\ddagger} = -RT \ln[(k_{cat}/K_m)_{mutant}/(k_{cat}/K_m)_{wild\ type}]$$

where R is the gas constant, T is the absolute temperature, k_{cat} is the turnover number, and K_m is the Michaelis constant (*25*).

K_i values for protease inhibition were determined by the method of progress curves, where reactions are initiated by addition of enzyme to a mixture of substrate and inhibitor (*20*, *26*). Reactions were conducted at 23 °C in 50 mM Tris (pH 7.4), 100 mM NaCl, and 1 mM EDTA. Inhibitor concentrations were varied and kept at a large excess over protease so that the inhibition reaction did not significantly deplete the free inhibitor. Apparent inhibition constants (K_{app}) were calculated from the relationship

$$v_0/v_i - 1 = [I]/K_{app}$$

where v_i is the steady state rate of substrate hydrolysis in the presence of inhibitor concentration [I] and v_0 is the uninhibited rate. K_i, the true equilibrium inhibition constant, was obtained by correcting K_{app} for the presence of substrate:

$$K_i = K_{app}/(1 + [S]/K_m)$$

where [S] is the substrate concentration and K_m is the Michaelis constant.

Differences in the free energy of inhibitor binding ($\Delta\Delta G$) for mutant proteases were calculated using the equation

$$\Delta\Delta G = -RT \ln[(K_i)_{\text{wild type}}/(K_i)_{\text{mutant}}]$$

where R is the gas constant, T is the absolute temperature, and K_i is the inhibition constant (*25*).

RESULTS AND DISCUSSION

Mutant Expression and Characterization. FAP mutant preparations were greater than 95% pure as assessed by SDS−PAGE and predominantly dimeric when analyzed by gel filtration chromatography and multiangle light scattering (Table 1 of the Supporting Information). To assess the effect of each mutation on FAP activity and specificity, we performed kinetic analyses with dipeptidyl peptidase (Gly-Pro-AFC) and endopeptidase (Ac-Gly-Pro-AFC) substrates.

FAP Requires Conserved DPP-4 Substrate-Binding Residues for Activity against Endopeptidase and Dipeptidyl Peptidase Substrates. We first assessed the function of FAP Arg^{123}, a conserved residue in DPP-4 that positions Glu^{205} for substrate binding and may additionally bind the P_2 carbonyl of dipeptidyl peptidase substrates (Figure 1A and refs *9*, *11*, *13*, and *14*). The R123A mutant exhibited significantly decreased activity against both endopeptidase and dipeptidyl peptidase substrates, demonstrating a 33-fold decrease in efficiency against Ac-Gly-Pro-AFC and a 5-fold decrease in catalytic efficiency against Gly-Pro-AFC relative to that of wild-type (WT) FAP (Table 1). In both cases, increased K_m and decreased k_{cat} values contributed to the low activity. Similar decreases in catalytic efficiency were observed for both substrates with R123M and R123K mutants, showing that FAP requires the positively charged guanidinyl group of Arg^{123} for optimal activity.

We next probed the function of FAP Glu^{203} and Glu^{204}, two conserved residues in DPP-4 that bind the positively charged N-terminus of dipeptidyl peptidase substrates (Figure 1A and refs *9*−*14*). As expected, mutation of these residues to Ala alone and in combination markedly diminished activity against the dipeptidyl peptidase substrate, Gly-Pro-AFC (Table 1). The catalytic efficiency for Gly-Pro-AFC cleavage decreased 60−81-fold for each single mutant (E203A and E204A) due to an increase in K_m and a marked decrease in k_{cat}. There was no detectable activity against Gly-Pro-AFC with the double mutant, E203/4A (1.5 mM substrate, 100 nM enzyme). Surprisingly, the E203A, E204A, and E203/4A mutants also had markedly reduced activity against the endopeptidase substrate, Ac-Gly-Pro-AFC, which lacks a positively charged N-terminus (Table 1). The single mutants (E203A and E204A) exhibited a 35−50-fold decrease in catalytic efficiency against Ac-Gly-Pro-AFC, due to increased K_m and decreased k_{cat} values. The double mutant E203/4A had an even greater loss of activity against Ac-Gly-Pro-AFC due to a large decrease in k_{cat}. Gln mutants (E203Q, E204Q, and E203/4Q) also exhibited marked decreases in catalytic efficiency against both substrate types, whereas Asp mutants (E203D, E204D, and E203/4D) partially restored activity against both substrates. Together, these data show that FAP activity requires the negatively charged carboxylate side chains of both Glu^{203} and Glu^{204}.

Table 1: Kinetic Constants for Substrate Hydrolysis by Conserved Active Site Residue Mutants[a]

protease	substrate	K_m (mM)	k_{cat} (s^{-1})	k_{cat}/K_m (M^{-1} s^{-1})
WT	GP-AFC	0.25	5.6	2.3×10^4 [b]
	Ac-GP-AFC	0.33	7.7	2.3×10^4 [b]
R123A	GP-AFC	0.38	1.7	4.5×10^3
	Ac-GP-AFC	0.67	0.47	701
R123M	GP-AFC	0.67	2.1	3.1×10^3
	Ac-GP-AFC	0.65	0.48	738
R123K	GP-AFC	1.1	1.2	1.1×10^3
	Ac-GP-AFC	0.48	0.4	833
E203A	GP-AFC	0.92	0.26	283
	Ac-GP-AFC	0.81	0.37	457
E204A	GP-AFC	0.73	0.28	384
	Ac-GP-AFC	0.69	0.45	652
E203/4A	GP-AFC	NC[c]	NC[c]	NC[c]
	Ac-GP-AFC	0.57	0.05	88
E203D	GP-AFC	0.44	0.19	432
	Ac-GP-AFC	0.1	0.36	3.6×10^3
E204D	GP-AFC	0.45	0.33	733
	Ac-GP-AFC	0.51	0.13	255
E203/4D	GP-AFC	0.55	0.71	1.3×10^3
	Ac-GP-AFC	0.14	1.4	1.0×10^4
E203Q	GP-AFC	1.8 ± 0.8	ND[d]	171[e]
	Ac-GP-AFC	2.3 ± 0.9	ND[d]	157[e]
E204Q	GP-AFC	0.75	0.19	253
	Ac-GP-AFC	0.74	0.60	811
E203/4Q	GP-AFC	1.5 ± 0.5	ND[d]	42[e]
	Ac-GP-AFC	1.4 ± 0.6	ND[d]	129[e]
Y656F	GP-AFC	1.1	0.15	136
	Ac-GP-AFC	0.84	0.37	440
N704A	GP-AFC	0.37	0.12	325
	Ac-GP-AFC	1.3 ± 0.6	ND[d]	4[e]

[a] The reported values represent the average of three or more independent experiments. Unless otherwise indicated, standard errors were <10%. [b] Values from ref *20*. [c] No cleavage. [d] Not determined. [e] Determined under first-order conditions.

To determine whether FAP activity requires Tyr^{656}, a conserved residue in DPP-4 that hydrogen bonds with the N-terminus of dipeptidyl peptidase substrates (Figure 1A and refs *9*−*14*), we measured the activity of a FAP Y656F mutant. This mutant had diminished activity against Gly-Pro-AFC due to an ~4-fold increase in K_m and a 37-fold decrease in k_{cat}. k_{cat} and K_m effects similarly reduced the catalytic efficiency of the mutant for Ac-Gly-Pro-AFC hydrolysis, indicating that FAP requires Tyr^{656} for dipeptidyl peptidase and endopeptidase activity.

Finally, we studied FAP Asn^{704}, a conserved residue in DPP-4 that binds the P_2 carbonyl of dipeptidyl peptidase substrates (Figure 1A and refs *9*, *11*, and *12*). Mutation of Asn^{704} to Ala diminished the catalytic efficiency of Gly-Pro-AFC hydrolysis more than 70-fold, largely due to a decrease in k_{cat} (Table 1). This mutant bound Ac-Gly-Pro-AFC weakly, which precluded a full Michaelis analysis. The catalytic efficiency determined under pseudo-first-order conditions was more than 2300-fold lower than the catalytic efficiency of WT FAP. Replacement of Asn^{704} with His, Gln, Asp, or Ser produced little dimeric enzyme (Table 1 of the Supporting Information), indicating that these substitutions are not tolerated and that FAP activity requires the size, polarity, and hydrogen bonding capacity of Asn^{704}.

Conserved Active Site Residues Stabilize the Enzyme−Substrate Transition. The reduced activity observed with the conserved residue mutants is consistent with their presumed

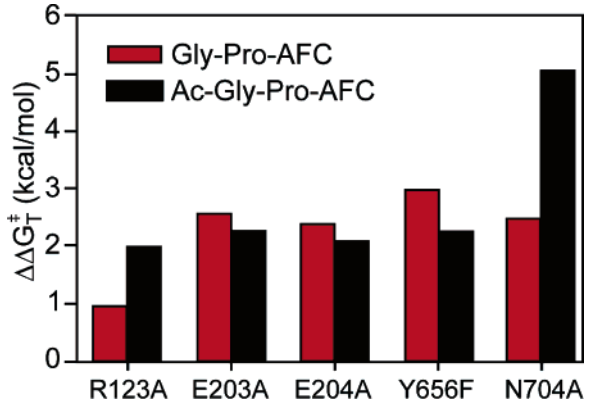

FIGURE 2: Changes in transition state binding energy ($\Delta\Delta G_T^{\ddagger}$) for dipeptidyl peptidase (Gly-Pro-AFC) and endopeptidase (Ac-Gly-Pro-AFC) substrates observed with conserved residue mutants.

role in substrate binding and further suggests that they stabilize transition state substrate binding. To assess this, we calculated losses in their transition state binding energy ($\Delta\Delta G_T^{\ddagger}$) relative to that of WT FAP (Figure 2). Decreases in binding energy were pronounced with both dipeptidyl peptidase and endopeptidase substrates, and their magnitude ($\Delta\Delta G_T^{\ddagger} = 1.0-5.1$ kcal/mol) suggests that the conserved residues stabilize transition state substrate binding via hydrogen bonding interactions (*27*). Interestingly, Glu^{203}, Glu^{204}, and Tyr^{656} stabilized binding of both substrates similarly; however, Arg^{123} and Asn^{704} provided greater stabilization for endopeptidase substrate binding.

FAP Endopeptidase Activity Requires Ala^{657}. We next focused on how Ala^{657} modulates endopeptidase activity because of a previous report implicating this residue in endopeptidase activity (*8*) and because our initial studies showed that seven other nonconserved residues near the active site are not important for endopeptidase specificity (Figure 1 and Table 2 of the Supporting Information).

To better understand how Ala^{657} permits FAP endopeptidase activity, we measured the activity of 10 different Ala^{657} mutants against Ac-Gly-Pro-AFC. Strikingly, all mutants had a significant decrease in endopeptidase activity relative to that of WT FAP, generally due to increased K_m values and decreased k_{cat} values (Table 2). Replacement of Ala^{657} with aliphatic (Val) or aromatic (Phe) residues decreased the catalytic efficiency of Ac-Gly-Pro-AFC cleavage by ~110- or >1600-fold, respectively. Substitution with smaller polar amino acids (Ser and Thr) decreased endopeptidase catalytic efficiency ~25−33-fold, whereas replacement with larger polar residues (Asn and Gln) or charged residues (Asp) profoundly slowed or abolished Ac-Gly-Pro-AFC hydrolysis. Substitution with Gly also resulted in low endopeptidase activity. Glu and Lys mutants were not active due to their inability to dimerize (Table 1 of the Supporting Information). Thus, FAP endopeptidase activity requires Ala at position 657.

The 10 Ala^{657} mutants were sorted into three groups based on dipeptidyl peptidase activity (Table 2). The first group (A657D and A657N) exhibited enhanced dipeptidyl peptidase activity relative to that of WT FAP. The A657D mutant markedly preferred Gly-Pro-AFC over Ac-Gly-Pro-AFC, showing a 10-fold increase in catalytic efficiency against Gly-Pro-AFC and a concomitant ~600-fold decrease in catalytic efficiency against Ac-Gly-Pro-AFC. The A657N mutant lacked activity against Ac-Gly-Pro-AFC but exhibited enhanced activity against Gly-Pro-AFC, suggesting that the carbonyl group of the Asp and Asn side chains is important for dipeptidyl peptidase activity. The second group (A657S, A657T, and A657Q) exhibited dipeptidyl peptidase activity similar to that of WT FAP but had diminished activity against the endopeptidase substrate. The final group (A657F, A657G, and A657V) had a marked decrease in activity against both substrates. Thus, several amino acid substitutions can support dipeptidyl peptidase activity, but FAP requires Ala at position 657 for endopeptidase activity.

Table 2: Kinetic Constants for Substrate Hydrolysis by FAP Ala^{657} Mutants[a]

group	mutant	substrate	K_m (mM)	k_{cat} (s^{-1})	k_{cat}/K_m (M^{-1} s^{-1})
WT	none	GP-AFC	0.25	5.6	2.3×10^4 [b]
		Ac-GP-AFC	0.33	7.7	2.3×10^4 [b]
higher DPP[f] activity	A657D	GP-AFC	0.062	14	2.3×10^5
		Ac-GP-AFC	0.78	0.03	39
	A657N	GP-AFC	0.087	8.9	1.0×10^5
		Ac-GP-AFC	NC[c]	NC[c]	NC[c]
WT DPP[f] activity	A657S	GP-AFC	0.135	4.7	3.5×10^4
		Ac-GP-AFC	0.52	0.46	885
	A657Q	GP-AFC	0.091	2.0	2.2×10^4
		Ac-GP-AFC	1.0 ± 0.2	0.09	90
	A657T	GP-AFC	0.11	4.5	4.1×10^4
		Ac-GP-AFC	0.42	0.29	690
lower DPP[f] activity	A657F	GP-AFC	0.41	0.20	488
		Ac-GP-AFC	1.3 ± 0.5	ND[d]	14[e]
	A657G	GP-AFC	1.3 ± 0.3	1.8	1.4×10^3
		Ac-GP-AFC	2.0 ± 0.6	ND[d]	182[e]
	A657V	GP-AFC	0.49	0.94	1.9×10^3
		Ac-GP-AFC	0.43	0.09	209

[a] The reported values represent the average of three or more independent experiments. Unless otherwise indicated, standard errors were <10%. [b] Values from ref *20*. [c] No cleavage. [d] Not determined. [e] Determined under first-order conditions. [f] Dipeptidyl peptidase.

Inhibition Studies with Transition State Analogues Define Distinct Roles for FAP Ala^{657} and DPP-4 Asp^{663}. The marked effects on protease activity observed with the Ala^{657} mutants suggest that Ala^{657}, like the conserved residues, stabilizes the enzyme−substrate transition state. The dramatic effects on FAP specificity observed with the A657D mutant further imply that FAP Ala^{657} and corresponding DPP-4 Asp^{663} modulate transition state stabilization differently. To test this hypothesis, we investigated the reactivity of WT and mutant (FAP A657D and DPP-4 D663A) proteases with transition state inhibitors.

We first tested protease reactivity with boronic acid inhibitors, which form a covalent boronate adduct with the active site serine (*28*, *29*) that mimics the tetrahedral intermediate of substrate hydrolysis (Figure 3). To model dipeptidyl peptidase and endopeptidase substrates, we used the proline-boronic acids (boroPro), Val-boroPro, Ile-boroPro, and Ac-Gly-boroPro. Small aliphatic residues (Val and Ile) were placed at P_2 instead of Gly for the dipeptidyl peptidase inhibitors since Gly-boroPro inactivates itself via intramolecular cyclization (*30*). Val-boroPro and Ile-boroPro inhibited FAP and the A657D mutant similarly, with K_i values in the low nanomolar range (Table 3). FAP also bound the endopeptidase inhibitor, Ac-Gly-boroPro, with nanomolar affinity. However, the A657D mutant bound Ac-Gly-boroPro weakly, having a K_i value 2000-fold greater than that of WT FAP. The boroPro compounds also inhibited DPP-4 and

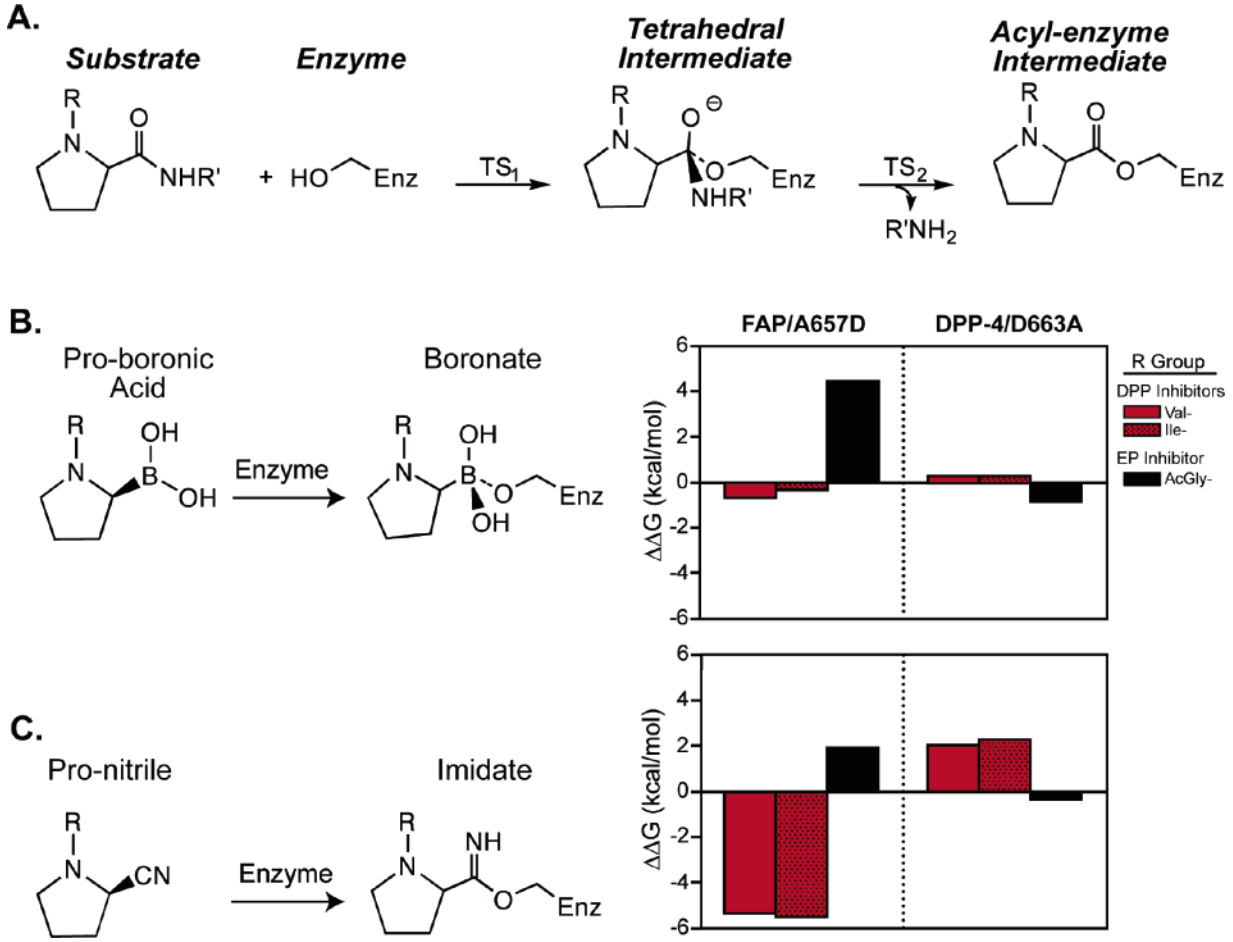

FIGURE 3: FAP Ala^{657} and DPP-4 Asp^{663} dictate the protease reaction with transition state analogues. (A) Initial steps of the serine protease reaction pathway. HO-Enz represents the catalytic serine. (B) Structure of a boroPro inhibitor and the tetrahedral boronate adduct. The graph shows changes in inhibitor binding energy ($\Delta\Delta G$) for the FAP A657D and DPP-4 D663A mutants. (C) Proline-nitrile inhibitor and the trigonal imidate adduct. The graph shows changes in inhibitor binding energy for the FAP A657D and DPP-4 D663A mutants. DPP stands for dipeptidyl peptidase and EP for endopeptidase.

Table 3: K_i Values (nanomolar) for Protease Inhibition by Proline-Boronic Acids[a]

	Val-boroPro	Ile-boroPro	Ac-Gly-boroPro
FAP	6.2 ± 0.1	14.0 ± 0.3	23 ± 3[b]
FAP A657D	2.2 ± 0.3	8.4 ± 0.6	$(4.6 \pm 0.3) \times 10^4$
DPP-4	0.17 ± 0.05	0.54 ± 0.10	377 ± 25[b]
DPP-4 D663A	0.28 ± 0.02	0.87 ± 0.20	85 ± 3

[a] The data represent the average $\pm$ the standard error of the mean for three or more independent experiments. [b] Data from ref *20*.

Table 4: K_i Values (nanomolar) for Protease Inhibition by Proline-Nitriles[a]

	Val-Pro-CN	Ile-Pro-CN	Ac-Gly-Pro-CN
FAP	$(3.4 \pm 0.1) \times 10^5$	$(8.4 \pm 0.2) \times 10^4$	$(6.8 \pm 0.4) \times 10^3$
FAP A657D	39.4 ± 1.4	7.8 ± 0.5	$(1.7 \pm 0.1) \times 10^5$
DPP-4	10.1 ± 0.6	1.9 ± 0.1	$(6.1 \pm 0.3) \times 10^4$
DPP-4 D663A	309 ± 19	89.6 ± 1.9	$(3.0 \pm 0.1) \times 10^4$

[a] The data represent the average $\pm$ the standard error of the mean for three or more independent experiments.

DPP-4 D663A, with the mutant showing moderately decreased affinity for Val-boroPro and Ile-boroPro and increased affinity for Ac-Gly-boroPro.

We next reacted each protease with an analogous set of proline-nitrile inhibitors, which form a covalent imidate adduct with the active site serine (*14*, *31*, *32*) that resembles the acyl−enzyme intermediate of substrate hydrolysis (Figure 3) (*28*). Surprisingly, these compounds inhibited FAP poorly with micromolar K_i values observed for both dipeptidyl peptidase (Val-Pro-CN and Ile-Pro-CN) and endopeptidase (Ac-Gly-Pro-CN) inhibitors (Table 4). In contrast, the A657D mutant bound Val-Pro-CN and Ile-Pro-CN much tighter (~8600−10700-fold decrease in K_i) and Ac-Gly-Pro-CN weaker (25-fold increase in K_i) than WT FAP. Val-Pro-CN and Ile-Pro-CN inhibited DPP-4 with low nanomolar K_i values, consistent with prior reports (*33*); however, Ac-Gly-Pro-CN inhibited DPP-4 with a micromolar K_i value. Relative to WT DPP-4, the D663A mutant bound Val-Pro-CN and Ile-Pro-CN weaker (~30−47-fold increase in K_i) and Ac-Gly-Pro-CN tighter (2-fold decrease in K_i).

To evaluate how introduction of Asp at FAP position 657 alters inhibitor binding energy, we calculated $\Delta\Delta G$ values for each inhibitor (Figure 3B,C). The Asp stabilized dipeptidyl peptidase inhibitor binding; however, stabilization was significantly greater with the proline-nitriles than the boroPros. In contrast, the Asp destabilized endopeptidase inhibitor binding, and greater destabilization was observed with the boroPro inhibitors. Substitution of DPP-4 Asp^{663} with Ala produced more moderate and opposite changes in inhibitor binding energies, and these were observed with both boroPro and proline-nitrile inhibitors (Figure 3). Thus, FAP Ala^{657} and DPP-4 Asp^{663} dictate the protease reaction with transition

state inhibitors, and this relates to their effects on the free energy of inhibitor binding.

FAP Substrate Binding Models. The mutagenesis data presented here support a direct role for the conserved residues in binding dipeptidyl peptidase and endopeptidase substrates. For dipeptidyl peptidase substrates, the substrate's positively charged N-terminus likely hydrogen bonds with the carboxylate side chains of Glu^{203} and Glu^{204}, as well as the phenolic hydroxyl group of Tyr^{656} as modeled in Figure 4A. The amide group of Asn^{704} forms a hydrogen bond with the substrate's P_2 carbonyl oxygen. Additionally, after a minor rotation, the carbonyl oxygen of the Asn side chain can hydrogen bond with the phenolic side chain of Tyr^{656}, which may position the Tyr residue optimally for substrate binding. Arg^{123} hydrogen bonds to Glu^{203}, and this likely positions the Glu residue optimally for substrate binding. Slight rotation of the Arg would also allow hydrogen bonding with the substrate's P_2 carbonyl oxygen. Similar binding interactions likely occur with endopeptidase substrates (Figure 4B), except that Glu^{203} and Glu^{204} bind the amide nitrogen of the P_2 Gly residue instead of the positively charged N-terminus of the dipeptidyl peptidase substrate (Figure 4A). Additionally, Tyr^{656} is too far removed from this amide nitrogen for hydrogen bonding and probably orients Glu^{204} optimally for substrate binding. Thus, the conserved residues bind both substrate types and orient the scissile bond for cleavage.

Although Ala^{657} also supports transition state binding of endopeptidase substrates, this residue does not bind substrate and likely regulates protease specificity by controlling the geometry of the active site. Consistent with this, the 4 Å distance between Ala^{657} and Glu^{204} (Figure 4B) allows the Glu residue more conformational freedom than the corresponding Asp residue in DPP-4 (Figure 4C). The methyl side chain of Ala^{657} likely provides Glu^{204} the ideal amount of conformational freedom for endopeptidase activity as substitution with larger or smaller amino acids markedly diminishes endopeptidase activity (Table 3). By contrast, the 2.5 Å distance separating DPP-4 Asp^{663} and Glu^{206} allows these residues to hydrogen bond (Figure 4C), which conformationally restrains Glu^{206} such that endopeptidase activity cannot occur.

FAP Inhibition Model. Besides regulating protease specificity, FAP Ala^{657} and DPP-4 Asp^{663} dictate the reaction with transition state analogues, with the Ala promoting reaction with boroPro inhibitors but limiting reaction with prolinenitrile inhibitors and the Asp permitting reaction with both inhibitors. To identify potential structural reasons for this, we docked these inhibitors into the FAP and DPP-4 active sites (Figure 5). The models suggest three potential factors responsible for the differences in protease inhibition. First, as observed with substrate binding, FAP Ala^{657} and DPP-4 Asp^{663} modulate the conformation of FAP Glu^{204} and DPP-4 Glu^{206}, which alters interaction of the conserved Glu residue with the inhibitor's N-terminus. Second, the tetrahedral geometry of the boroPro adduct and trigonal nature of the imidate adduct lead to slight differences in the positioning of the inhibitors, which alters their contact with the conserved active site residues. Third, the hydroxyl groups of the boroPro inhibitor hydrogen bond with Tyr^{541} and His^{734} (Figure 5A), but the imidate nitrogen hydrogen bonds with only His^{734}. It is likely that this additional hydrogen bonding, the highly electrophilic nature of the boron atom, and the aforementioned differences in the geometry of the inhibitor−protease adducts all contribute to FAP's higher-affinity binding of boroPro inhibitors.

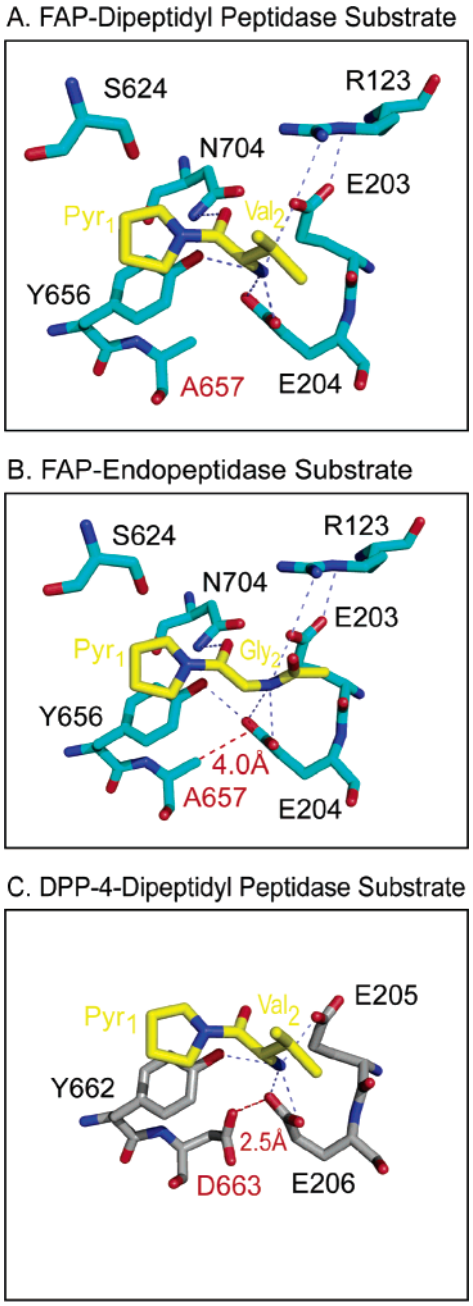

FIGURE 4: FAP substrate binding models. (A) Model for binding of the dipeptidyl peptidase substrate Val-pyrrolidide to FAP based on our data, the FAP crystal structure [PDB entry 1z68 (*8*)] and the DPP-4 crystal structure with bound inhibitor [PDB entry 1n1m (*9*)]. The same color scheme that was used in Figure 1C was used here. The position of the catalytic serine, Ser^{624}, is indicated at the top left. (B) Model for binding of the endopeptidase substrate to FAP. Ac-Gly-pyrrolidide, which models an endopeptidase substrate, is docked into the FAP active site. The red dashed line highlights the 4 Å distance separating the side chains of Ala^{657} and Glu^{204}, which allows Glu^{204} considerable conformational freedom. (C) Structure of DPP-4 bound to the dipeptidyl peptidase inhibitor Val-pyrrolidide with a shorter distance (2.5 Å) between DPP-4 Asp^{663} and Glu^{206} (red dashed line). This allows these residues to hydrogen bond, which conformationally restrains Glu^{206}.

Although DPP-4 Asp^{663} stabilized dipeptidyl peptidase inhibitor binding, it markedly destabilized endopeptidase inhibitor binding. The Asp does not sterically hinder binding

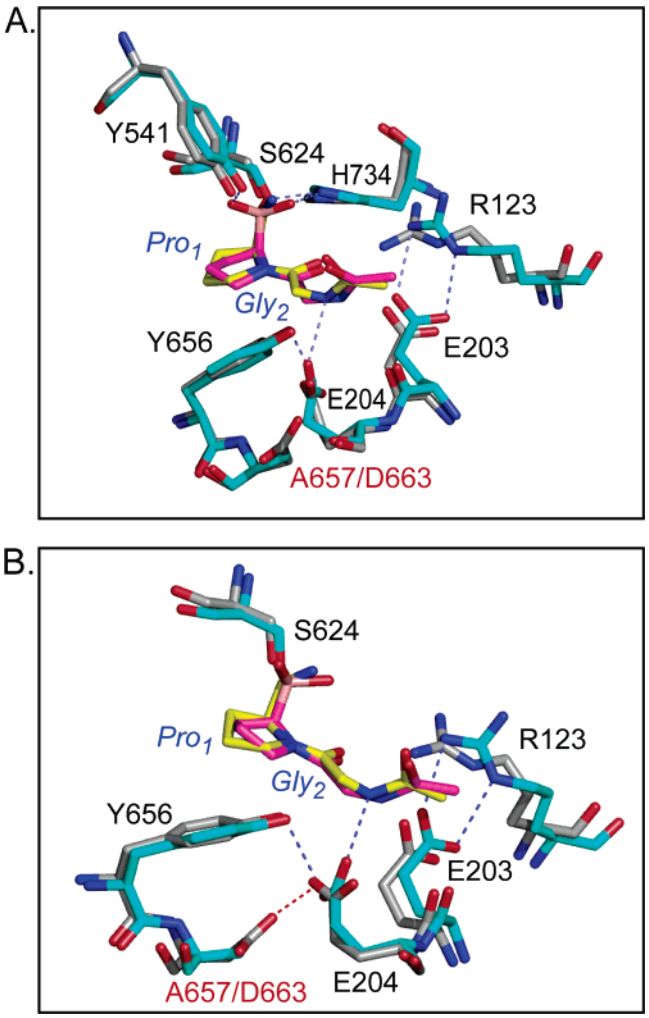

FIGURE 5: FAP inhibition models. (A and B) Two views of proline-nitrile (Ac-Gly-Pro-CN; yellow) and boroPro (Ac-Gly-boroPro; pink) inhibitors docked into the FAP (cyan) and DPP-4 (gray) active sites. The models are based on the FAP structure [PDB entry 1z68 (*8*)] and the structure of DPP-4−inhibitor complexes [PDB entries 2gbf (*31*) and 2ajd (*29*)]. Selected hydrogen bonds are shown as dashed lines.

of the inhibitor to the DPP-4 active site (Figure 5), suggesting that the nature of the carboxylate side chain destabilizes binding. The carboxylate's hydrogen bonding capacity likely allows binding and deprotonation of the Glu^{206} side chain, and the resultant negative charge strongly disfavors binding of uncharged endopeptidase substrates or inhibitors. This implies that avoidance of unsolvated charge drives dipeptidyl peptidase versus endopeptidase specificity and that N-blocked inhibitors like Ac-Gly-boroPro should preferentially inhibit FAP relative to DPP-4-like proteases. Indeed, Ac-Gly-boroPro shows marked selectivity against DPP-8 and DPP-9 [K_i 8800−19100-fold greater than that of FAP (*20*)], prolyl peptidases that share DPP-4's Glu-Asp dyad and exhibit DPP-4-like substrate specificity (*34*). Future studies with these prolyl peptidases should expand our understanding of the structure−activity relationship of N-acyl-Gly-boroPro inhibitors and aid in selective inhibitor design.

ACKNOWLEDGMENT

We thank Bob Lazarus for critically reading the manuscript and Janie Pena for graphics support.

SUPPORTING INFORMATION AVAILABLE

Data (two tables and one figure) on mutagenesis primers, protein dimer content, and additional mutants. This material is available free of charge via the Internet at http://pubs.acs.org.

REFERENCES

1. Rosenblum, J. S., and Kozarich, J. W. (2003) Prolyl peptidases: A serine protease subfamily with high potential for drug discovery, *Curr. Opin. Chem. Biol. 7*, 496−504.
2. Demuth, H.-U., McIntosh, C. H. S., and Pederson, R. A. (2005) Type 2 diabetes: Therapy with dipeptidyl peptidase IV inhibitors, *Biochim. Biophys. Acta 1751*, 33−44.
3. Garin-Chesa, P., Old, L. J., and Rettig, W. J. (1990) Cell surface glycoprotein of reactive stromal fibroblasts as a potential antibody target in human epithelial cancers, *Proc. Natl. Acad. Sci. U.S.A. 87*, 7235−7239.
4. Scanlan, M. J., Mohan, B. K. M., Calvo, B., Garin-Chesa, P., Sanz-Moncasi, M. P., Healey, J. H., Old, L. J., and Rettig, W. J. (1994) Molecular cloning of fibroblast activation protein α, a member of the serine protease family selectively expressed in stromal fibroblasts of epithelial cancers, *Proc. Natl. Acad. Sci. U.S.A. 91*, 5657−5661.
5. Dolznig, H., Schweifer, N., Puri, C., Kraut, N., Rettig, W. J., Kerjaschki, D., and Garin-Chesa, P. (2005) Characterization of cancer stroma markers: In silico analysis of mRNA expression database for fibroblast activation protein and endosialin, *Cancer Immun. 5*, 1−10.
6. Cheng, J. D., Dunbrack, R. L., Valianou, M., Rogarto, A., Aplaugh, R. K., and Weiner, L. M. (2002) Promotion of tumor growth by murine fibroblast activation protein, a serine protease, in an animal model, *Cancer Res. 62*, 4767−4772.
7. Huang, Y., Wang, S., and Kelly, T. (2004) Seprase promotes rapid tumor growth and increased microvessel density in a mouse model of human breast cancer, *Cancer Res. 64*, 2712−2716.
8. Aertgeerts, K., Levin, I., Shi, L., Snell, G. P., Jennings, A., Prasad, G. S., Zhang, Y., Kraus, M. L., Salakian, S., Sridhar, V., Wijnands, R., and Tennant, M. G. (2005) Structural and kinetic analysis of the substrate specificty of human fibroblast activation protein α, *J. Biol. Chem. 280*, 19441−19444.
9. Rasmussen, H. B., Branner, S., Wiberg, F. C., and Wagtmann, N. (2003) Crystal structure of human dipeptidyl peptidase IV/CD26 in complex with a substrate analog, *Nat. Struct. Biol. 10*, 19−25.
10. Thoma, R., Loffler, B., Stihle, M., Huber, W., Ruf, A., and Henning, M. (2003) Structural basis of proline-specific exopeptidase activity as observed in human dipeptidyl peptidase-IV, *Structure 11*, 947−959.
11. Engel, M., Hoffmann, T., Wagner, L., Wermann, M., Heiser, U., Kiefersauer, R., Huber, R., Bode, W., Demuth, H.-U., and Brandstetter, H. (2003) The crystal structure of dipeptidyl peptidase IV (CD26) reveals its functional regulation and enzymatic mechanism, *Proc. Natl. Acad. Sci. U.S.A. 100*, 5063−5068.
12. Aertgeerts, K., Ye, S., Tennant, M. G., Kraus, M. L., Rogers, J., Sang, B.-C., Skene, R. J., Webb, D. R., and Prasad, G. S. (2004) Crystal structure of human dipeptidyl peptidase IV in complex with a decapeptide reveals details on substrate specificity and tetrahedral intermediate formation, *Protein Sci. 13*, 1−10.
13. Hiramatsu, H., Yamamotoa, A., Higashiyama, Y., Fukushima, C., Shima, H., Sugiyama, S., Inaka, K., and Shimizu, R. (2004) The cyrystal structure of human dipeptidyl peptidase IV (DPPIV) complex with diprotin A, *Biol. Chem. 385*, 561−564.
14. Oefner, C., D'Arcy, A., Mac Sweeney, A., Pierau, S., Gardiner, R., and Dale, G. (2003) High resolution structure of human apo dipeptidyl peptidase IV/CD26 and its complex with 1-[((2-[(5-iodopyridin-2-yl-amino]-ethyl]amino)acetyl]-2−2cyano-(S)-pyrrolidine, *Acta Crystallogr. D59*, 1206−1212.
15. Pineiro-Sanchez, M., Goldstein, L., Dodt, J., Howard, L., Yeh, Y., and Chen, W.-T. (1997) Identification of the 170-kDa melanoma membrane-bound gelatinase (Seprase) as a serine integral membrane protease, *J. Biol. Chem. 272*, 7595−7601.
16. Park, J. E., Lenter, M. C., Zimmermann, R. N., Garin-Chesa, P., Old, L. J., and Rettig, W. J. (1999) Fibroblast activation protein, a dual specificity serine protease expressed in reactive human tumor stromal fibroblasts, *J. Biol. Chem. 274*, 36505−36512.

17. Chien, C., Huang, L., Chou, C., Chen, Y., Han, Y., Chang, G., Liang, P., and Chen, X. (2004) One site mutation disrupt dimer formation in human DPP-IV proteins, *J. Biol. Chem. 279*, 52338−52345.
18. Edosada, C., Quan, C., Tran, T., Pham, V., Wiesmann, C., Fairbrother, W., and Wolf, B. (2006) Peptide substrate profiling defines fibroblast activation protein as an endopeptidase of strict Gly_2-Pro_1-cleaving specificity, *FEBS Lett. 580*, 1581−1586.
19. Yoshimoto, T., Fischl, M., Orlowski, R., and Walter, R. (1978) Post-proline cleaving enzyme and post-proline dipeptidyl aminopeptidase, *J. Biol. Chem. 253*, 3708−3716.
20. Edosada, C., Quan, C., Wiesmann, C., Tran, T., Sutherlin, D., Reynolds, M., Elliott, J., Raab, H., Fairbrother, W., and Wolf, B. (2006) Selective inhibition of fibroblast activation protein protease based on dipeptide substrate specificity, *J. Biol. Chem. 281*, 7437−7444.
21. Abbott, C., McCaughan, G., and Gorrell, M. (1999) Two highly conserved glutamic acid residues in the predicted β propeller domain of dipeptidyl peptidase IV are required for its enzyme activity, *FEBS Lett. 458*, 278−284.
22. Wang, X., Yu, D., McCaughan, G., and Gorrell, M. (2005) Fibroblast activation protein increases apoptosis, cell adhesion, and migration by the LX-2 human stellate line, *Hepatology 42*, 935−945.
23. Gibson, F., Singh, A., Soumeillant, M., Manchand, P., Humora, M., and Kronenthal, D. (2002) A practical synthesis of L-valylpyrrolidine-(2R)-boronic acid: Effecient recycling of the costly chiral auxiliary (+)-pinanediol, *Org. Process Res. Dev. 6*, 814−816.
24. Villhauer, E., Brinkman, J., Naderi, G., Burkey, B., Dunning, B., Prasad, K., Mangold, B., Russell, M., and Hughes, T. (2003) 1-[[(3-Hydroxy-1-adamantyl)-amino]acetyl]-2-cyano-(S)-pyrrolidine: A potent, selective, and orally bioavailable dipeptidyl peptidase IV inhibitior with antihyperglycemic properties, *J. Med. Chem. 46*, 2774−2789.
25. Wells, J. (1990) Additivity of mutational effects in proteins, *Biochemistry 29*, 8509−8517.
26. Nicklin, M., and Barrett, A. (1984) Inhibition of cysteine proteinases and dipeptidyl peptidase I by egg-white cystatin, *Biochem. J. 223*, 245−253.
27. Fersht, A., Shi, J., Knill-Jones, J., Lowe, D., Wilkinson, A., Blow, D., Brick, P., Carter, P., Waye, M., and Winter, G. (1985) Hydrogen bonding and biological specificty analysed by protein engineering, *Nature 314*, 235−238.
28. Hedstrom, L. (2002) Serine protease mechanism and specificity, *Chem. Rev. 102*, 4501−4523.
29. Engel, M., Hoffmann, T., Manhart, S., Heiser, U., Chambre, S., Huber, R., Demuth, H.-U., and Bode, W. (2006) Rigidity and flexibility of dipeptidyl peptidase IV: Crystal structures of and docking experiments with DPIV, *J. Mol. Biol. 355*, 768−783.
30. Coutts, S., Kelly, T., Snow, R., Kennedy, C., Barton, R., Adams, J., Krolikowski, D., Freeman, D., Campbell, S., Ksiazek, J., and Bachovchin, W. W. (1996) Structure-activity relationships of boronic acid inhibitors of dipeptidyl peptidase IV. 1. Variation of the P_2 position of Xaa-boroPro dipeptides, *J. Med. Chem. 39*, 2087−2094.
31. Longenecker, K., Stewart, K., Madar, D., Jakob, C., Fry, E., Wilk, S., Lin, C., Ballaron, S., Stashko, M., Lubben, T., Yong, H., Pireh, D., Pei, Z., Basha, F., Wiedeman, P., von Geldern, T., Trevillyan, J., and Stoll, V. (2006) Crystal structures of DPP-IV (CD26) from rat kidney exhibit flexible accomodation of peptidase-selective inhibitors, *Biochemistry 45*, 7474−7482.
32. Wright, S., Ammirati, M., Andrews, K., Brodeur, A., Danley, D., Doran, S., Lillquist, J., McClure, L., McPherson, R., Orena, S., Parker, J., Polivkova, J., Qiu, X., Soeller, W., Soglia, C., Treadway, J., VanVolkenburg, M., Wang, H., Wilder, D., and Olson, T. (2006) *cis*-2,5-Dicyanopyrrolidine inhibitors of dipeptidyl peptidase IV: Synthesis and in vitro, in vivo, and X-ray crytallographic characterization, *J. Med. Chem. 49*, 3068−3076.
33. Ashworth, D., Atrash, B., Baker, G., Baxter, A., Jenkins, P., Jones, D., and Szelke, M. (1996) 2-Cyanopyrrolidides as potent, stable inhibitors of dipeptidyl peptidase IV, *Bioorg. Med. Chem. Lett. 6*, 1163−1166.
34. Bjelke, J., Christensen, J., Nielsen, P., Branner, S., Kanstrup, A., Wagtmann, N., and Rasmussen, H. B. (2006) Dipeptidyl peptidases 8 and 9: Specificity and molecular characterization compared with dipeptidyl peptidase IV, *Biochem. J. 396*, 391−399.

BI062227Y